Int. J. Environ. Sci. Technol. (2013) 10:465–472
DOI 10.1007/s13762-012-0111-1

ORIGINAL PAPER

Municipal solid waste incineration fly ash sintered lightweight aggregates and kinetics model establishment

W. F. Tan · L. A. Wang · C. Huang · J. E. Green

Received: 4 November 2011 / Revised: 22 May 2012 / Accepted: 9 October 2012 / Published online: 9 November 2012

Abstract Municipal solid waste incineration fly ash blended with pine sawdust and shale, using a neotype trefoil rotary kiln to form lightweight aggregates, is an effective and a potential means method of fly ash disposal. The optimum sintering conditions of Trefoil rotary kiln were determined in terms of an orthogonal test by measuring the pellets' bulk density, granule strength, 1 h water absorption. As far as the kinetics is concerned, an integral method of Coats–Redfern was introduced to analyze the kinetics characteristics of the mixture samples. Also, the kinetic triplets (apparent activation energy, pre-exponential factor and reaction order) were estimated by the reaction of kinetics model functions. It is shown that the optimum sintering conditions are as follows: (a) preheating temperature of 500 °C, (b) sintering temperature of 1130 °C, (c) holding time of 4 min. The optimum reaction models of the four stages are Avrami–Erofeev, Mample, Avrami–Erofeev and There-dimensional diffusion (Jander), respectively.

W. F. Tan · L. A. Wang (✉) · C. Huang
State Key Laboratory of Coal Mine Disaster Dynamics and Control, College of Resources and Environmental Science, Chongqing University, No. 174 Shazhengjie, Shapingba, Chongqing 400044, China
e-mail: wang65111477@yahoo.com.cn

W. F. Tan
e-mail: 470642773@qq.com

C. Huang
e-mail: hclsjb@163.com

J. E. Green
Sustainability Research Institute, University of East London, London, UK
e-mail: j.e.green@uel.ac.uk

Keywords Fly ash · Pine sawdust · Shale · Lightweight aggregates · Kinetics model

Introduction

Traditional ways of MSW disposal include landfill, compost and incineration. Incineration with its merits of site selection flexibility, large capacity, fast processing speed, volume reduction and recyclable energy, etc., currently, has seen rapid development and extensive use in China. However, the new environment puzzle is how to deal with the incineration fly ash which is classified as a hazardous waste, and has received substantial attention all over the world (Zhang and Zhao 2010), principally owe to its high chloride content and significant amounts of leachable heavy metals (lead, Pb, Zn, etc.).

In recent years, various technologies have been investigated to reduce the hazardous characteristics of MSWI fly ash (Abanades and Flamant 2002; Raungrut and Chai 2004; Silitonga et al. 2009; Wang et al. 2010; Zhang et al. 2008; Zhang and Zhao 2007). These researches have laid a good foundation for the disposal and recycling of MSWI fly ash. However, it is difficult to remove polychlorinated dibenzofurans and dibenzop-dioxins, and effectively eliminate the heavy metals from MSWI fly ash. Also, paper from Taiwan has used metal sludge mixed with mining residues to be recycled into lightweight aggregate (Chang et al. 2007); a recent work from Spain has utilized mining and industrial waste to produce lightweight aggregate (González-Corrochano et al. 2011). However, there are rarely publicly reports for the MSWI fly ash as main raw material to form lightweight aggregate.

This work emphasizes the utilization of fly ash as a raw material to form lightweight aggregates. It not only limits

the use of natural resources and still satisfies the growing demand for aggregate, but also creates an economical perspective for fly ash.

In this study, aiming to reduce the generation of PCDD/Fs from the source, chloride, the prerequisite for generating PCDD/Fs (Cieplik et al. 2006) in MSWI fly ash was decreased by way of a preliminary washing treatment with water. Process water can be recycled, and then discharged with neutralization. In addition, the contents of Cd, Cr, Cu, Zn and Pb in the MSWI fly ash were analyzed by a sequential chemical extraction procedure with $HCl/HNO_3/HF/HClO_4$ and Hg with $HCl/H_2O_2/HNO_3$, and the leaching toxicity of heavy metals in the lightweight aggregates was tested by AAS. Moreover, to understand the thermal reaction process, an integral method of Coats–Redfern was introduced to analyze the kinetics parameters and to study thermal reaction mechanism of MSWI fly ash, pine sawdust and shale based on TG-DSC curve. The thermodynamic models that give the best linear fit were selected as the reaction mechanism function.

Materials and methods

Experimental site

The fly ash used in this study was sampled from tongxing MSW Incineration Plant, Chongqing, China, which was firstly dried at 105 °C for 24 h to constant weight, then washed with distilled water at a liquid-to-solid ratio (L/S) of 10:1. Finally, the residues were dried and stored for sintering. Shale used to increase the proportion of aluminosilicate came from a suburb of Chongqing, and sludge used as an expanding agent from the Jiguanshi wastewater treatment plant, Chongqing, China. The specific processes are shown in Fig. 1:

- Washed fly ash together with grinded shale and sludge were mixed with water, controlling moisture content of mixture to approximately 30 %.
- The mixture was used in the manufacture of pellets in a granulator, followed by oven drying for 5 h at 105 °C.
- The baked pellets were put into the trefoil rotary kiln at 500 °C. The speed of rotation of the kiln was controlled at 7–10 r/min. The pellets were sintered for approximately 20 min until the temperature rose to 1130 °C, at which point, it was maintained for 2–6 min, and then the heat was stopped. When the kiln cooled to 1000 °C, the ceramic pellets were removed and allowed to cool to room temperature before testing the parameters of the ceramic pellets.

Analysis methods of raw materials

X-ray fluorescence analyzer (XRF): the Shimadzu XRF-1800, testing conditions were Rh target, 40 kV, 95 mA, 20°/min.

X-ray diffraction (XRD): the BDX3200, testing conditions were Cu target, 40 kV, 100 mA, scanning speed 2°/min.

The leaching toxicity analysis was performed by means of HJ/T 300-2007, 10 g of the fly ash sample was immersed in 200 ml of 1.725 % anhydrous acetic acid solution diluted with deionized water and shaken for 18 ± 2 h on an oscillating flip style device. In the last step, using AAS (AA6000) analyze the leaching toxicity of heavy metals according with GB/T 5085.3-2007 standard. The contents of Cd, Cr, Cu, Zn and Pb in the residue were analyzed by a sequential chemical extraction procedure with $HCl/HNO_3/HF/HClO_4$ and Hg with $HCl/H_2O_2/HNO_3$.

DSC-TG analysis: NETZSCH STA 449C thermal instrument was used to analyze the mixture: fly ash, sawdust and shale, the crucible material was Al_2O_3, carrier gas

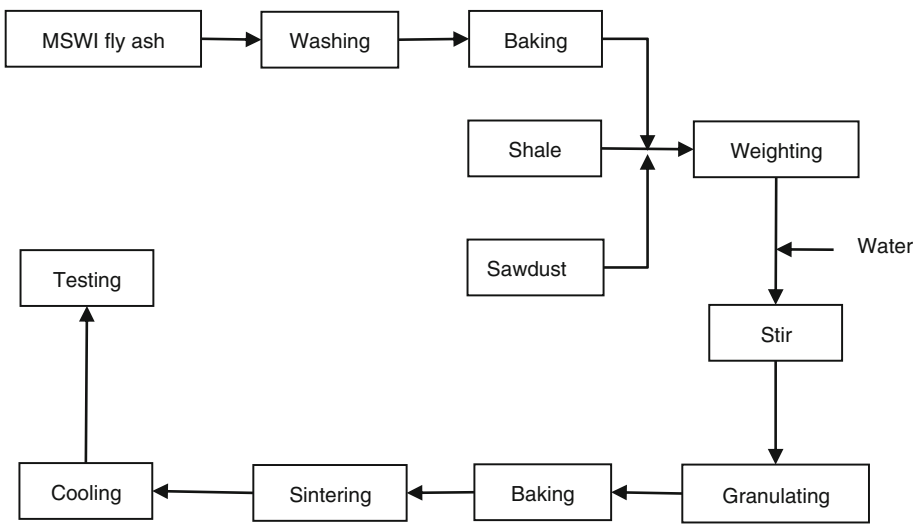

Fig. 1 Experimental technology process

Table 1 The orthogonal test

Level	Factor		
	A Preheating temperature/°C	B Sintering temperature/°C	C Holding time/min
1	450	1100	2
2	500	1130	4
3	550	1160	6

type and flow rate of air 50 mL/min, shielding gas and flow rate of Ar10 mL/min, heating rates was 20 K/min, temperature range was 25–1200 °C.

Main experimental apparatus

The Trefoil rotary kiln mimics the rock formation of the natural volcanic eruption process. The inner cylinder of the Kiln has a corrugated design, so it can rapidly heat and cool lightweight aggregates and melt toxic substances effectively, reducing the generation of volatile toxic gases significantly.

Compared with the traditional rotary kiln, the trefoil rotary kiln has a higher thermal efficiency. Aerospace alloy steel was used as the inner wall, soft thin steel as the outer wall, and ceramic fiber as the heat insulation film located between the aerospace alloy steel and the soft thin steel, forming a three-lobed, box-shaped cross section.

Orthogonal test

A 3-level 3-factor orthogonal test shown in Table 1 was performed to determine the optimal sintering parameters. Granules made by the optimal mixture ratio were characterized and assessed for bulk density, granule strength and 1 h water absorption.

Results and discussion

Chemical composition analysis

Chemical composition of raw materials was presented in Table 2 (XRF). The compounds of original fly ash mainly contain SiO_3, CaO, Al_2O_3, Fe_2O_3, Na_2O, and K_2O. After water washing pretreatment, the amount of Na, K, etc., soluble-salts were significantly reduced. The proportion of Si and Ca doubled to 13.9 and 50.3 %, respectively. Shale which contains as much as 69.77 wt.% of the SiO_3+Al_2O_3, was used to increase the proportion of aluminosilicate. Sawdust which contains a lot of hydrocarbons was selected as an expanding agent.

Figure 2 (XRD) shows that phase composition of original fly ash is much complex. The crystal types found in MSWI fly ash contain mainly KCl(41-1476), NaCl(05-0628), CaSO4(37-1496), K2Mg2(SO4)3(19-0974), CaCO3 (05-0586), SiO2(16-1045), MgAl(SiAlO5)(52-1569), Ca2Al2 SiO7(35-0755), NaSi3AlO8(10-0393), Ca(OH)2(44-1481), etc., Fig. 3 indicated that mineral constitutions of MSWI fly ash changed after water washing pre-treatment. Most of the chlorine was washed off during the water washing process mainly due to the significant reduction of soluble salt—NaCl and KCl.

Orthogonal test

Washing pretreatment fly ash, pine sawdust and shale were blended with a proper mix ratio orthogonal test. Bulk density, granule strength and 1 h water absorption were chosen as measurement criteria. The results were shown in Table 3. In this experiment, a quadratic regression analysis of experimental data with DPS software was used to analyze the test results shown in Table 4, to obtain the optimal performance of lightweight aggregates.

As the variance analysis of experimental results in Table 4 shows:

- In terms of bulk density, the optimal combination of sintering process is A2-B3-C3. As the sintering temperature and holding time decreased, the bulk density of pellets increased gradually. This is because when the pellets reach a certain temperature, the surface began to liquefy. Within the selected temperature range, as the temperature continues to increase, the surface of the pellets liquid also increased; while the combustion gas of the internal residual carbon continued to escape through the surface of liquid and forms the internal

Table 2 Chemical composition analysis of raw materials (wt.%)

Samples	SiO_2	Fe_2O_3	Al_2O_3	CaO	MgO	Na_2O	K_2O	SO_3	Ignition loss	Caloricity
Fly ash	26.14	5.32	9.19	21.95	3.32	5	5.97	2.86	27.08	154 J
Washed fly ash	13.95	3.7	3.78	50.32	4.74	0.99	0.88	10.11	23.38	117 J
Shale	50.40	15.84	19.37	5.38	1.18	0.86	2.44	0.92	4.13	–
Sawdust	–	–	–	–	–	–	–	–	99.72	17420 J

The chemical composition of the three materials were analyzed by XRF, also, Ignition loss and Caloricity are shown in this table

– not tested

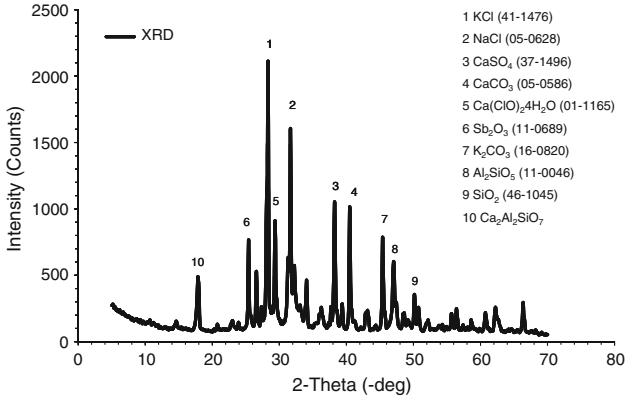

Fig. 2 XRD spectrum analysis of original fly ash (X-ray diffraction (XRD): the BDX3200; testing conditions were: Cu target, 40 kV, 100 mA, scanning speed 2°/min)

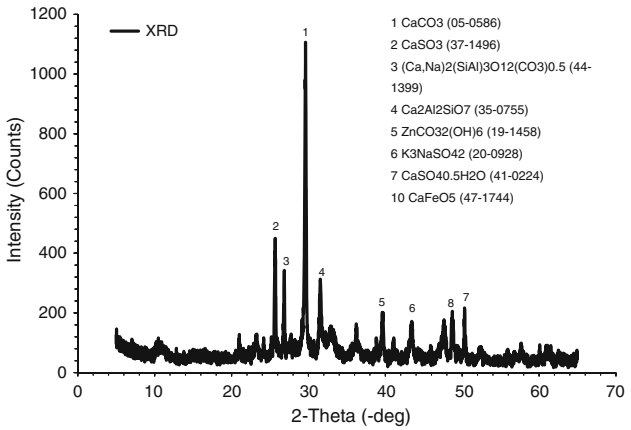

Fig. 3 XRD spectrum analysis of washed fly ash (X-ray diffraction (XRD): the BDX3200; testing conditions were: Cu target, 40 kV, 100 mA, scanning speed 2°/min)

Table 3 Results of orthogonal test

No.	A	B	C	Bulk density (kg m^{-3})	Granule strength (*N*)	1 h water absorption (%)
1	1	1	1	708	532	16.77
2	1	2	2	670	695	12.39
3	1	3	3	613	782	13.64
4	2	1	2	683	551	14.11
5	2	2	3	646	628	12.23
6	2	3	1	631	826	11.89
7	3	1	3	684	463	20.35
8	3	2	2	658	659	15.77
9	3	3	1	620	924	10.73

porous hollow structure, so that the bulk density of ceramic pellets decreased.

- In terms of granule strength, the optimal combination of sintering process is A2-B3-C2. Within the selected temperature range, as the temperature continues to increase, the surface of the pellets liquid also increased gradually. However, as the holding time increased, there was an initial increase in intensity before it began to decrease. This is because as the sintering temperature is kept at 1160 °C above 6 min, the internal formation of pellets structure of interconnected pores forms a large pore structure, making the granule strength of ceramic pellets decrease.
- In terms of 1 h water absorption, the optimal combination of sintering process is A2-B3-C2. As the sintering temperature, which is a significant factor, increased, the water absorption decreased. This is mainly because, as the sintering temperature increased, more and more liquid wrapped the surface, gradually forming a layer of impermeable surface-enamel membrane leading to a reduction in the water absorption of the ceramic pellets.

To sum up, considering the energy and the performance of lightweight aggregates, the optimum sintering conditions were determined as follows: (a) preheating temperature of kiln is 500 °C, (b) sintering temperature is 1130 °C, (c) holding time is 4 min. In accordance with the optimal sintering conditions, a great many granules (4 kg) were sintered using the trefoil rotary kiln to form lightweight aggregates, sample appearances are shown in Fig. 4.

Pore structure of lightweight aggregates surface is few and far between and materials in a glassy phase occupy most of the granule surface. Compared with the lightweight aggregates surface, the internal microstructure was completely different. Abundant pore structure was uniformly distributed within the internal granule. The different pore structure of the surface and interior formed a high strength, low water absorbing lightweight aggregate.

Leaching toxicity analysis

The leaching toxicity analysis was performed by means of HJ/T 300-2007(solid waste-extraction procedure for leaching toxicity-Acetic acid buffer solution method): 10 g of the fly ash sample was immersed in 200 ml of 1.725 % anhydrous acetic acid solution diluted with deionized water and shaken for 18 ± 2 h on an oscillating flip style device. In the last step, using AAS analyze the leaching toxicity of heavy metals. The total heavy metals content and the leaching toxicity were listed in Table 5. The results showed that the lead heavy metals were Cd, Cr, Hg, Cu, Pb, Zn, and Hg, and the content of Pb and Zn exceeded the limit described in "Identification standard of hazardous waste–identification of leaching toxicity" (GB5085.3-2007) which adversely affect the environment. The remaining five heavy metals can meet the leaching limit value. Combined with the leaching toxicity of lightweight aggregate, the heavy metal extraction

Table 4 Experimental results of variance analysis

	Bulk density (kg m^{-3})			Granule strength (*N*)			1 h water absorption (%)		
	A	B	C	A	B	C	A	B	C
Kj1	1,991	2,075	1,997	2,009	1,546	2,017	42.80	51.23	44.43
Kj2	1,960	1,974	1,973	2,005	1,982	2,170	38.23	40.38	37.23
Kj3	1,962	1,864	1,943	2,046	2,532	1,873	46.85	36.26	46.21
K1	663.67	691.67	665.67	669.67	515.33	672.33	14.27	17.08	14.81
K2	653.33	658.00	657.67	668.33	660.67	723.33	12.74	13.46	12.41
K3	654.00	621.33	647.67	682.00	844.00	624.33	15.62	12.09	15.40
Extremum	10.34	70.34	18	13.67	328.67	99	2.88	4.99	2.99
Optimal choice	A_2	B_3	C_3	A_2	B_3	C_2	A_2	B_3	C_2

The experimental result of variance analysis was shown in the table. The optimum sintering conditions were determined by comparing the performance of lightweight aggregates

Fig. 4 Appearance and section of lightweight aggregates (In accordance with the optimal sintering conditions, a great many granules (4 kg) were sintered using the trefoil rotary kiln to form lightweight aggregates, sample appearances are shown in this figure)

value are obvious reductions. Among them, the content of Cd, Cr, Hg in the leach liquor cannot be detected, and the content of the other four heavy metals: Cu is 0.5, Pb is 0.03 and Zn is 0.8 mg/L, respectively. In general, there are two possibilities of heavy metals during the sintering process, volatilization and stabilization. The volatile portion was collected into the flue gas collection system. The second fly ash after cooling was recycled and the gas was purified, thereby ensuring the stability of discharge standards. As to difficult volatile heavy metals, Cd, Cr, Cu, Zn, during the sintering process, it was wrapped or trapped into a new phase structure. Acid extractables which jeopardize human and the environment mostly transformed to another three speciation—iron oxide occluded, organically bounded and residua are relatively stable. For volatile heavy metals, Pb, Hg, most were transformed to another three speciation, while the rest small part were collected and treated by gas collection system. In addition, the content of chlorine (The prerequisite for generating PCDD/Fs) in raw fly ash and washed fly ash was analyzed. Raw fly ash contains nearly 21 % of Chlorine. After the pretreatment of water washing, the Cl was reduced to a percentage of only 1.4 % compared with the original fly ash, leading to a reduction in the amount of Dioxins which could be generated during the sintering and the cooling process. Hence, washing pretreatment of MSWI fly ash is an effective way to remove chlorine.

TG-DSC analysis

A sync analyzer of thermogravimetry (TG) and differential scanning calorimetry (DSC) were simultaneously employed for testing parameters of the mixture to analyze the combustion kinetics parameters and the changing of lattice during sintering process of raw materials. The TG curve reflects the variation trend of the mixture weight with the temperature increasing. The DSC curve reflects the endothermic/exothermic chemical process. Figure 5 represents the TG-DSC curves of the mixture.

The whole sintering process can be generally divided into four stages. The stage 1 was identified in the

Table 5 Heavy metals leaching toxicity and elementary analysis of fly ash

Samples	Leaching toxicity (mg/L)							Elementary analysis (wt.%)
	Cd	Cr	Cu	Pb*	Zn*	Hg		Cl
Total content of fly ash	61.65	575.87	748.62	1158.44	5594.03	22.08	Raw fly ash	21.0
Leaching toxicity of fly ash	0.165	2.64	4.18	10.68	157.31	0.018		
Leaching toxicity lightweight aggregate	–	–	0.5	0.03	0.8	–	Washed fly ash	1.4
Leaching toxicity standard (GB 5085.3-2007)	≤1	≤15	≤100	≤5	≤100	≤0.2		

* Leaching toxicity exceeded the standard limit (GB5085.3-2007)

– Means undetected

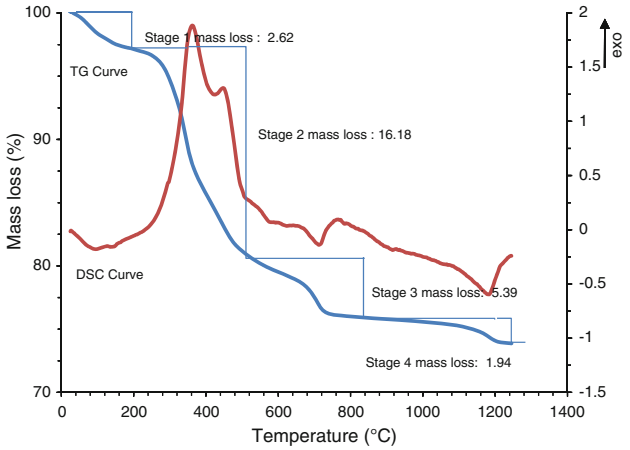

Fig. 5 TG-DSC curves analysis for the mixture (The TG curve reflects the variation trend of the mixture weight with the temperature increasing. The DSC curve reflects the endothermic/exothermic chemical process)

temperature 25–120 °C with a total mass loss of 2.62 %, it can be speculated that the moisture and highly volatile matters evaporated at this stage. The stage 2 and stage 3, where the main mass loss occurred, were identified in the temperature 120–750 °C with a total mass loss of 16.18 and 5.39 %, respectively. Combined with the DSC curve, a large exothermic peak appeared in the stage 2 and it can be speculated that the sawdust burned at this stage. Moreover, a endothermic peak appeared in the stage 3 due to heat absorbed by easily decomposed compounds, such as $Ca(OH)_2$. The stage 4 was identified above 1000 °C with a total mass loss of 1.94 %. Combined with the DSC curve, an endothermic peak appeared at this stage, and it can be speculated that the calcite or residues were decomposed at this stage.

Fundamental rationale

The general information of the pyrolysis process is shown in the TG-DSC curves. In this paper, Coats–Redfern integral method without neglecting the low-temperature end of the temperature integral (Coats and Redfern 1964; Cai and Bi 2008), based on the approximation of temperature integral, has been used to analyze the kinetics of non-isothermal processes. In each pyrolysis phase, the rate of a solid-state reaction can be generally described by:

$$\frac{d\alpha}{dt} = \frac{A}{\beta}\exp\left(-\frac{E}{RT}\right)f(\alpha) \tag{1}$$

where A is the pre-exponential (frequency) factor, E is the activation energy, T is absolute temperature, R is the universal gas constant, β is the heating rate, $f(\alpha)$ is the reaction model, and is the conversion fraction. For a gravimetric measurement, α is defined by:

$$\alpha = \frac{m_0 - m_t}{m_0 - m_\infty} \tag{2}$$

where m_0 is initial weight, m_t is weight at time t, and m_∞ is final weight.

Integration both sides of Eq. (1) for α from 0 to α and T from T_0 to T, respectively, using $G(\alpha)$ instead of $\int_0^\alpha \frac{1}{f(\alpha)}d\alpha$, then a method neglecting the low-temperature end of the temperature integral from Coats–Redfern can be described by:

$$G(\alpha) = \frac{A}{\beta}\int_0^\alpha \exp\left(-\frac{E}{RT}\right)dT \tag{3}$$

and a method without neglecting the low-temperature end of the temperature integral from Junmeng Cai and Lianshan Bi can be described by:

$$G(\alpha) = \frac{A}{\beta}\left(\int_0^T \exp\left(-\frac{E}{RT}\right)dT - \int_0^{T_0} \exp\left(-\frac{E}{RT}\right)dT\right) \tag{4}$$

Equations (3) and (4) has no analytical solution, but has many approximations (Chen and Lai 2004) with one of the most popular being the Coats–Redfern method. This method utilizes the asymptotic series expansion for

Table 6 Commonly used solid-state reaction kinetics model functions

Reaction model	Symbol	$f(\alpha)$	$g(\alpha)$
Phase interface reaction	Rn	$n(1-\alpha)^{1-1/n}$	$1-(1-\alpha)^{1/n}$
Ample	F1	$1-\alpha$	$\ln(1-\alpha)$
Avrami–Erofeev	Am	$m(1-\alpha)[-\ln(1-\alpha)]^{1/(1-m)}$	$[-\ln(1-\alpha)]^{1/m}$ ($m = 1/2, 1/3, 1/4$)
One-dimensional diffusion	D1	$(1/2)\alpha^{-1}$	α^2
Two-dimensional diffusion	D2	$-1/\ln(1-\alpha)$	$\alpha+(1-\alpha)\ln(1-\alpha)$
There-dimensional diffusion (Jander)	D3	$3(1-\alpha)^{2/3}/\{2[1-(1-\alpha)^{-1/3}]\}$	$[1-(1-\alpha)^{1/3}]^2$
There-dimensional diffusion (Ginstring–Brounshtein)	D4	$3/\{2[(1-\alpha)^{-1/3}-1]\}$	$1-(2\alpha/3)-(1-\alpha)^{2/3}$

approximating the exponential integral. By virtue of Eqs. (3) and (4), respectively, the equation for the determination of the apparent activation energy can be obtained from the slope of the plot of $\ln\frac{G(\alpha)}{T^2}$ versus $1/T$:

$$\frac{d\ln\left[G(\alpha)/T^2\right]}{d\left(1/T\right)} = -\frac{E_a}{R}\left[1-\frac{2}{E_a/RT\left(E_a/RT-2\right)}\right] \tag{5}$$

The equation for the determination of the true activation energy can be obtained from the slope of the plot of $\ln\left[\frac{G(\alpha)}{T^2}\right]$ versus $1/T$:

$$\frac{d\ln\left[G(\alpha)/T^2\right]}{d\left(1/T\right)} = 2T + \frac{d\ln\left[\int_{T_0}^{T}\exp\left(-E_t/RT\right)dT\right]}{d(1/T)} \tag{6}$$

Introducing the parameter $\gamma = E/RT_0$ (a dimensionless activation energy) and the variable $\zeta = T/T_0$ (the normalized temperature), Eq. (6) can be expressed as follows:

$$\frac{d\ln\left[G(\alpha)/T^2\right]}{d(1/T)} = \frac{E}{R}\left\{2\frac{\zeta}{\gamma} - \frac{\zeta^2 d\ln\left[\int_1^{\zeta}\exp(-\gamma/\zeta)d\zeta\right]}{\gamma d\zeta}\right\} \tag{7}$$

The relative error of the activation energy can be defined by the following equation:

$$\varepsilon = \frac{E_a - E_t}{E_t} \tag{8}$$

Then the relative error of the activation energy can be obtained by:

$$-(\varepsilon+1)\left\{1-\frac{2}{(\varepsilon+1)\gamma/\zeta\left[(\varepsilon+1)\gamma/\zeta-2\right]}\right\} = 2\frac{\gamma}{\zeta} - \frac{\zeta^2 d\ln\left[\int_1^{\zeta}\exp\left(-\gamma/\zeta\right)d\zeta\right]}{\gamma d\zeta} \tag{9}$$

Using the values of α and T from TG experiment, a graph of left hand side of $\ln\left[\frac{G(\alpha)}{T^2}\right]$ can be plotted versus $1/T$. The plot should result in a series of data points close to a straight line. Regression analysis with least square fitting method is used to find the equation of the straight line and plot it to evaluate the values of E and A. Detailed information about the calculated process can be found in the literature of Cai and Bi.

Kinetics parameters and reaction mechanism

In this paper, the kinetic triplets (apparent activation energy, pre-exponential factor and reaction order) were estimated by the reaction kinetics model functions. Table 6

Table 7 Kinetics parameters analysis and model establishment

Temperature range/(°C)	Reaction Model	$g(\alpha)$	Fit equation	r	E_t/(kJ/mol)	A_t/(min^{-1})	n
25–120	Am	$[-\ln(1-\alpha)]^4$	y = − 22996x − 52.46	0.982	182.5	7.13e-018	4
271–501	F1	$-\ln(1-\alpha)$	y = −7877x − 1.296	0.931	62.84	46221	1
680–734	Am	$[-\ln(1-\alpha)]^2$	y = − 160600x + 149.2	0.972	1320.4	1.86e + 071	2
1100–1200	D3	$[1-(1-\alpha)^{1/3}]^2$	y = −173900x + 103.2	0.959	1419.7	2.12e + 051	2

Through the comparison of fitting results of the above reaction kinetics model functions, the best linear fitting degree function was chosen as the combustion reaction mechanism function for the corresponding phase. The kinetic parameters obtained from the non-linear regression equation were shown in this table

has listed the commonly used solid-state reaction kinetics model functions (Hu et al. 2008).

Through the comparison of fitting results of the above reaction kinetics model functions, the best linear fitting degree function was chosen as the combustion reaction mechanism function for the corresponding phase (Otero et al. 2007). The kinetic parameters obtained from the non-linear regression equation were shown in Table 7.

The model that gives the best linear fit is selected as the chosen model. As seen from fitting results in Table 7, the optimum reaction models of the four stages are Avrami–Erofeev, Mample, Avrami–Erofeev and There-dimensional Diffusion (Jander), respectively. The E and A values of the stage 1 and stage 2 are much lower than that of stage 3 and stage 4. Combined with the TG-DSC analysis of the above, we can draw the conclusion that the moisture evaporated and the sawdust burned need lower activation energy of the calcite and residues decomposed.

Conclusion

This paper provides a method of making an economically useful commercial synthetic aggregate, utilizing a substantial portion of MSWI fly ash sintered in the trefoil rotary kiln. Also, the kinetic triplets were estimated by the reaction kinetics model functions. The results of these experiments have led us to conclude the following:

- The optimal sintering parameters: (a) preheating temperature of 500 °C in the kiln, (b) sintering temperature of 1,130 °C, (c) holding time of 4 min
- There are two possibilities of heavy metals during the sintering process, volatilization and stabilization. The volatile portion was collected into the flue gas collection system. The second fly ash after cooling was recycled and the gas was purified, thereby ensuring the stability of discharge standards.
- The sintering process including four reaction stages: (a) moisture volatile, (b) volatile and semivolatile organic matter precipitation, (c) refractory organic matter and fixed carbon combustion, (d) calcite and relicts decomposition.
- The optimum reaction models of the four stages are Avrami–Erofeev, Mample, Avrami–Erofeev and There-dimensional Diffusion (Jander), respectively, also, the E and A values of the stage 1 and stage 2 are much lower than that of stage 3 and stage 4.

Acknowledgments The research work was funded by Science & Technology Committee, Chongqing, project number-CSTC.2011 AC7065, and Technical cooperation of the RTAL Company, Hong-Kong. Hereby, all the support is greatly appreciated.

References

Abanades S, Flamant G (2002) Fate of heavy metals during municipal solid waste incineration. Waste Manage 20:55–68

Cai JM, Bi LS (2008) Precision of the Coats and Redfern method for the determination of the activation energy without neglecting the low-temperature end of the temperature integral. Energy Fuels 22:2172–2174

Chen HJ, Lai KM (2004) Methods for determining the kinetics parameters from nonisothermal thermogravimetry. J Chem Eng Japan 37(9):1172–1178

Cieplik MK, DeJong V, Bozovic J (2006) Formation of dioxins from combustion micropollutants over MSWI fly ash. Environ Sci Technol 40:1263–1269

Coats A, Redfern J (1964) Kinetic parameters from thermogravimetric data. Nature Publishing Group, London

Chang F-C, Lo S-L, Lee M-Y, Ko C-H, Lin J-D, Huang S-C, Wang C-F (2007) Leachability of metals from sludge-based artificial lightweight aggregate. J Hazard Mater 146:98–105

González-Corrochano B, Alonso-Azcárate J, Rodas-Gonzalez M (2011) Heavy metal chemical fractionation and immobilization in lightweight aggregates produced from mining and industrial waste. Int J Environ Sci Technol 8(4):667–676

Hu RZ, Gao SL, Zhao FQ, Shi QZ, Zhang TL, Zhang JJ (2008) Thermal analysis kinetics. Science Press, Beijing

Otero M, Gomez X, Garcia AI, Moran A (2007) Effects of sewage sludge blending on the coal combustion a thermogravimetric assessment. Chemosphere 69:1740–1750

Raungrut C, Chai J (2004) A study of disposed fly ash from landfill to replace Portland cement. Waste Manage 24:701–709

Silitonga E, Levacher D, Mezazigh S (2009) Effects of the use of fly ash as a binder on the mechanical behavior of treated dredged sediments. Environ Technol 30(8):799–807

Wang JH, Chang LP, Li F, Xie KC (2010) A study on the combustion properties of western Chinese coals. Energy Sources Part A: Recovery Utilization and Environmental Effects 11:1040–1051

Zhang HY, Zhao YC (2007) Study on use of MSWI fly ash in ceramic tile. J Hazard Mater 141:106–114

Zhang HY, Zhao YC (2010) Utilization of municipal solid waste incineration (MSWI) fly ash in ceramic brick: product characterization and environmental toxicity. Waste Manage 31:331–341

Zhang HJ, Yu Y, Ni YW (2008) Stabilization of heavy metals in municipal solid waste incineration fly ash with the thiol collectors. J Environ Sci 28:1899–1904